

# New composite models of partially ionized protoplanetary disks

Caroline E. J. M. L. J. Terquem<sup>1</sup>

*Institut d'Astrophysique de Paris, UMR 7095 CNRS, Université Pierre & Marie Curie Paris 06, 98 bis bd  
Arago, 75014 Paris, France  
caroline.terquem@iap.fr*

## ABSTRACT

We study an accretion disk in which three different regions may coexist: MHD turbulent regions, dead zones and gravitationally unstable regions. Although the dead zones are stable, there is some transport due to the Reynolds stress associated with waves emitted from the turbulent layers. We model the transport in each of the different regions by its own  $\alpha$  parameter, this being 10 to  $10^3$  times smaller in dead zones than in active layers. In gravitationally unstable regions,  $\alpha$  is determined by the fact that the disk self-adjusts to a state of marginal stability. We construct steady-state models of such disks. We find that for uniform mass flow, the disk has to be more massive, hotter and thicker at the radii where there is a dead zone. In disks in which the dead zone is very massive, gravitational instabilities are present. Whether such models are realistic or not depends on whether hydrodynamical fluctuations driven by the turbulent layers can penetrate all the way inside the dead zone. This may be more easily achieved when the ratio of the mass of the active layer to that of the dead zone is relatively large, which in our models corresponds to  $\alpha$  in the dead zone being about 10% of  $\alpha$  in the active layers. If the disk is at some stage of its evolution not in steady-state, then the surface density will evolve toward the steady-state solution. However, if  $\alpha$  in the dead zone is much smaller than in the active zone, the timescale for the parts of the disk beyond a few AU to reach steady-state may become longer than the disk lifetime. Steady-state disks with dead zones are a more favorable environment for planet formation than standard disks, since the dead zone is typically 10 times more massive than a corresponding turbulent zone at the same location.

*Subject headings:* accretion, accretion disks — planetary systems: protoplanetary disks — stars: pre-main sequence

## 1. Introduction

Protoplanetary disks are believed to have a complex structure. In the parts which are ionized enough (*active zones*), the magnetic field couples to the gas and the magnetorotational instability (MRI; Balbus & Hawley 1991) develops, leading to turbulence and angular momentum transport. Some parts however are too cold and dense for the ionization to reach the level required for MHD turbulence to be sustained. However, in these so-called *dead zones*, there may still be some low level of transport due to Reynolds or non turbulent

Maxwell stresses (Fleming & Stone 2003, Turner & Sano 2008). Finally, parts of the disk may be dense enough that gravitational instabilities develop, redistributing mass and angular momentum in such a way that the disk settles into a state of marginal stability. To date, there is no numerical simulations of such global disks. Global three dimensional MHD simulations so far have modeled stratified and fully turbulent disks, but with no dead zones (Fromang & Nelson 2006).

It is of interest to study whether non-uniform disks composed of different regions as described above can be in steady-state or not. Previous studies (Gammie 1999, Armitage et al. 2001)

<sup>1</sup>Institut Universitaire de France

assumed that no transport at all took place in the dead zone. Therefore mass could only pile-up there until gravitational instabilities would develop. If the level of transport is non zero in the dead zone however, the disk may be able to adjust to reach a steady-state. It is this possibility that we investigate in this paper.

In determining the characteristics of the disk vertical structure, we ignore reprocessing of the stellar radiation. Only heating associated with the different (magnetic and hydrodynamic) stresses is considered. Reprocessing has been shown to be important when the disk surface is flared (Kenyon & Hartmann 1987, Chiang & Goldreich 1997, D'Alessio et al. 1998, Dullemond et al. 2001). It provides an extra heating source that dominates the disk beyond a few AU and has important consequences on the structure of the dead zone (Matsumura & Pudritz 2006). However, in the models we present below, the parts of the disk beyond 1 AU are shielded from the stellar radiation by the inner parts. These models, which do not include reprocessing, are therefore self-consistent.

The plan of the paper is as follows. In section 2 we describe the way we model the transport in a disk with turbulent regions, dead zones and gravitationally unstable regions. In section 3 we present the equations governing the disk vertical structure and describe how they are solved. In section 4 we present the results of the calculations, and discuss them in section 5. We find that steady-state solutions exist and correspond to disks which are thicker, hotter and more massive than disks without dead zones.

## 2. Modeling of the disk transport

Protoplanetary disks are almost certainly magnetized, as they form from molecular clouds which are observed to contain a magnetic field. If the magnetic pressure is smaller than the thermal pressure, then the parts of the disk where the field couples to the gas are prone to the MRI. Its non-linear development is turbulence that transports angular momentum outward and therefore enables accretion (Hawley et al. 1995, Brandenburg et al. 1995). Recent numerical simulations of the MRI in shearing-boxes have shown that the level of transport depends on the Prandtl number (ratio of the viscosity to the resistivity; Fromang et al. 2007,

Lesur & Longaretti 2007). The simulations, which have not converged yet, also show that the turbulence is not sustained when the net magnetic flux is zero and for the range of parameters investigated (relatively large Prandtl numbers). It is reasonable to suppose that the magnetic field in protoplanetary disks does not vary very much on the scale of a few scale heights. For this reason, and if these disks were to be described locally by a shearing box, it would be more appropriate to assume a finite net flux. In the parts of the disk that are coupled to the field, we will therefore assume that turbulence is sustained and quantify the angular momentum transport using the parametrization of Shakura & Sunyaev (1973), with  $\alpha_T$  being the ratio of the stress to the pressure (the subscript 'T' refers to turbulence). It has been shown that this prescription, which is formally valid only if the disk evolves under the action of a viscosity, can be used to describe the global properties and evolution of MHD turbulent disks, although details and stability issues cannot be studied within this framework (Balbus & Papaloizou 1999). Given that  $\alpha_T$  as measured in the simulations depends on the Prandtl number, and that Prandtl numbers typical of protoplanetary disks are way too small to be investigated numerically, we will assign values to  $\alpha_T$  based on observations. The diffusion timescale is indeed limited by the disk lifetime, which is observed to be of a few  $10^6$  years. This implies  $\alpha_T \sim 10^{-3}$ – $10^{-2}$  (at least in the outer parts of the disk which are fully turbulent).

In protoplanetary disks, the minimum ionization fraction which is required for MHD turbulence to be initiated and sustained is on the order of  $10^{-13}$  on scales of 1 AU (e.g., Balbus & Hawley 2000). Although very small, this level of ionization is not reached in some parts of the disks, which are relatively cold and dense. The extent of the dead zone has been computed by several authors, taking into account ionization by cosmic rays (Gammie 1996, Sano et al. 2000 who also included radioactivity) and X-rays (Igea & Glassgold 1999, Fromang et al. 2002, Matsumura & Pudritz 2003 who also included cosmic rays and radioactivity). In this paper, we will denote by  $\Sigma_T$  the surface density of the active layer, i.e. the surface density beyond which ionizing photons cannot penetrate. Depending on the energy of these photons,  $\Sigma_T$  may vary in the range 10–100 g cm $^{-2}$

(Gammie 1996, Fromang et al. 2002). Note that the ionization in the disk inner parts is thermal, with the most abundant ions being  $\text{Na}^+$  and  $\text{K}^+$ . For the ionization fraction to be larger than  $10^{-13}$ , the temperature has to be higher than some value  $T_i$  which is close to  $10^3$  K over a large range of densities (Balbus & Hawley 2000). There is evidence from numerical simulations that some level of transport can be present in a dead zone that is sandwiched in between turbulent layers (Fleming & Stone 2003), as the turbulence drives hydrodynamic waves that propagate in the dead zone and are associated with a Reynolds stress. More recently, Turner & Sano (2008) have also proposed that magnetic field be able to diffuse from the active layers into the dead zone. Although the resistivity there is too high for MHD turbulence to be sustained, there is a large scale magnetic stress associated with the field that drives accretion. (If dust grains are present in the disk however, the magnetic field may not be able to diffuse down to the disk midplane at all radii.) The transport and energy deposition in the dead zone due to these stresses are non local. However, for illustrative purposes, we will parameterize this transport with a Shakura & Sunyaev parameter that we will denote  $\alpha_D$  (where the subscript 'D' refers to dead zone). Fleming & Stone (2003) found that the Reynolds stress in the dead zone is about 10% of the Maxwell stress in the active layers. Normalized by the thermal pressure, this translates into  $\alpha_D$  being between 0.07 and 0.3 times  $\alpha_T$ . However, in their simulations, the mass of the dead zone was only a few times that of the active layer. We might expect lower values of the Reynolds stress deep into the dead zone when the mass of the active layer is significantly smaller than that of the active zone, which is the case in the models we present below. Therefore, we will take  $\alpha_D$  in the range  $10^{-3}\alpha_T - 10^{-1}\alpha_T$ .

In the parts of the disk which are dense and cold, gravitational instabilities develop. Spiral density waves grow and transport angular momentum outward and mass inward. The level of saturation is determined by the fact that the disk settles into a state of marginal stability, with the Toomre parameter  $Q$  being on the order of 1.5 (Laughlin & Bodenheimer 1994, Lodato & Rice 2004). It was shown by Balbus & Papaloizou (1999) that in general, in a gravitation-

ally unstable disk, the transport is non local and cannot be described using the viscous disk theory. However, these authors pointed out that a local transport model might apply if the disk maintains itself in a state of marginal stability, which is the case considered here. In the regions where the disk is gravitationally unstable, we will therefore use the Shakura & Sunyaev prescription and will adjust the transport parameter, that we will denote  $\alpha_G$  (where the subscript 'G' refers to gravity), such as to have  $Q \sim 1.5$ .

It is important to keep in mind that here the disk is modeled in a very schematic way. We believe this does not affect the gross features of the models we present below, although the details should be considered with caution.

### 3. Disk vertical structure

We consider a system of cylindrical coordinates  $(r, \varphi, z)$  based on the central star, with  $z = 0$  being the disk midplane.  $P$  is the pressure,  $\rho$  is the mass density per unit volume,  $T$  is the temperature,  $\Omega$  is the angular velocity,  $\nu$  is the 'enhanced' kinematic viscosity associated with  $\alpha_T$  in turbulent layers,  $\alpha_D$  in dead zones and  $\alpha_G$  in gravitationally unstable regions, and  $\kappa$  is the opacity, which in general depends on both  $\rho$  and  $T$ . The thin-disk approximation is used throughout (and checked to be valid *a posteriori*), so that  $\Omega^2 = GM_\star/r^3$ ,  $M_\star$  being the mass of the central star and  $G$  the gravitational constant.

The disk vertical structure is described by the equation of vertical hydrostatic equilibrium:

$$\frac{1}{\rho} \frac{\partial P}{\partial z} = -\Omega^2 z, \quad (1)$$

together with the energy equation, which states that the rate of energy removal by radiation is locally balanced by the rate of energy production by viscous dissipation:

$$\frac{\partial F}{\partial z} = \frac{9}{4} \rho \nu \Omega^2 = \frac{9}{4} \alpha \Omega P, \quad (2)$$

where  $F$  is the radiative flux of energy through a surface of constant  $z$ . To write the last term of this equation, we have used  $\nu = \alpha c_s^2 / \Omega$ , where  $c_s = (P/\rho)^{1/2}$  is the isothermal sound speed and  $\alpha = \alpha_T$  in active layers,  $\alpha = \alpha_D$  in dead zones and  $\alpha = \alpha_G$  in the gravitationally unstable parts

of the disk. Therefore  $\alpha$  is a function of both  $z$  and  $r$ . The flux  $F$  is given by:

$$F = \frac{-16\sigma T^3}{3\kappa\rho} \frac{\partial T}{\partial z}, \quad (3)$$

with  $\sigma$  being the Stefan–Boltzmann constant. In principle, equation (3) is valid only at radii where the disk is optically thick. However, when the disk is optically thin, i.e. when  $\kappa\rho$  integrated over the disk thickness is small compared to unity, the temperature gradient given by equation (3) is small, so that the results we get are consistent in that case also. To close the system of equations, we adopt the equation of state of an ideal gas:

$$P = \frac{\rho k T}{2m_H}, \quad (4)$$

where  $k$  is the Boltzmann constant and  $2m_H$  is the mass of the hydrogen molecule, which is the main component of protostellar disks at the temperatures and densities of interest here.

### 3.1. Boundary conditions

We have to solve three first order ordinary differential equations for the three variables  $F$ ,  $P$  (or equivalently  $\rho$ ), and  $T$  as a function of  $z$  at a given radius  $r$ . Accordingly, we need three boundary conditions at each  $r$ . These have been described in detail in Papaloizou & Terquem (1999), so here we just recall briefly their expression. We denote with a subscript  $s$  values at the disk surface. The flux at the surface is given by:

$$F_s = \frac{3}{8\pi} \dot{M} \Omega^2, \quad (5)$$

where  $\dot{M} = 3\pi \langle \nu \rangle \Sigma$ , with  $\Sigma = \int_{-H}^H \rho dz$  being the disk surface mass density and  $\langle \nu \rangle = \int_{-H}^H \rho \nu dz / \Sigma$  being the vertically averaged viscosity. If the disk is in a steady state,  $\dot{M}$  does not vary with  $r$  and is the constant accretion rate through the disk.  $H$  and  $-H$  are the upper and lower boundaries of the disk, respectively. The surface pressure is given by:

$$P_s = \frac{\Omega^2 H \tau_{ab}}{\kappa_s}, \quad (6)$$

where  $\tau_{ab}$  is the optical depth above the disk. Since we have defined the disk surface such that

the atmosphere above the disk is isothermal, we have to take  $\tau_{ab} \ll 1$ . Providing this is satisfied, the results do not depend on the value of  $\tau_{ab}$  we choose (see Papaloizou & Terquem 1999). Finally, the surface temperature satisfies the following equation:

$$2\sigma (T_s^4 - T_b^4) - \frac{9\alpha_s k T_s \Omega}{8\mu m_H \kappa_s} - \frac{3}{8\pi} \dot{M} \Omega^2 = 0. \quad (7)$$

Here the disk is assumed immersed in a medium with background temperature  $T_b$ , so that the surface temperature remains finite.

### 3.2. Model Calculations

We look for steady-state solutions, so that  $\dot{M}$  does not depend on  $r$ . At a given  $r$  we then solve equations (1), (2) and (3) with the boundary conditions (5), (6) and (7) to find the dependence of the state variables on  $z$ . The (Rosseland) opacity is taken from Bell & Lin (1994). This has contributions from dust grains, molecules, atoms and ions. It is written in the form  $\kappa = \kappa_i \rho^a T^b$  where  $\kappa_i$ ,  $a$  and  $b$  vary with temperature. To carry out the integration, we start from an estimated value of  $H$  and iterate until the condition  $F = 0$  at  $z = 0$  is satisfied (see details in Papaloizou & Terquem 1999). The integration starts at  $z = H$ , where we have  $\alpha = \alpha_T$ , assuming the disk is not gravitationally unstable, and proceeds all the way down to  $z = 0$ . At each value of  $z$ , we compute  $\Sigma(z) = \int_z^H \rho(z') dz'$  and compare it with  $\Sigma_T$ . When  $\Sigma(z) > \Sigma_T$ , and if  $T(z) < T_i$ , we fix  $\alpha = \alpha_D$ . Once the vertical integration is finished, we calculate the Toomre parameter  $Q = c_s \Omega / \pi G \Sigma$ , where  $\Sigma$  is now the total surface density and  $c_s$  is evaluated at the midplane. When  $Q < 1.5$ , we increase  $\alpha$ , that we now call  $\alpha_G$ , slightly, assume that it is now independent of  $z$ , and redo the integration. We iterate the calculation, increasing  $\alpha_G$  at each step, until  $Q$  becomes larger than 1.5. As the step with which we increase  $\alpha_G$  has a finite size, we usually end up with a value of  $Q$  between 1.5 and 2 after at most 20 iterations.

In the calculations presented here, we have taken  $M_\star = 1 M_\odot$ ,  $T_i = 10^3$  K, the optical depth of the atmosphere above the disk surface  $\tau_{ab} = 10^{-2}$  and a background temperature  $T_b = 10$  K.

In the optically thick regions of the disk, the value of  $H$  is independent of the value of  $\tau_{ab}$  we choose. This is not the case in optically thin regions where we find that, as expected, the smaller  $\tau_{ab}$ , the larger  $H$ . However, this dependence of  $H$  on  $\tau_{ab}$  has no physical significance, since the surface mass density, the optical thickness through the disk and the midplane temperature hardly vary with  $\tau_{ab}$ . This is because the mass is concentrated towards the disk midplane in a layer with thickness independent of  $\tau_{ab}$ .

#### 4. Results

In figure 1, we plot  $H/r$  versus  $r$  (from 0.05 to 100 AU) for  $\dot{M} = 10^{-8} M_{\odot} \text{ yr}^{-1}$ ,  $\alpha_T = 10^{-2}$ ,  $\alpha_D = 10^{-4}$  and  $\Sigma_T = 10$  and  $50 \text{ g cm}^{-2}$ . The solid line delimits the surface of the disk whereas the dotted lines delimit the different regions in the disk. For  $\Sigma_T = 10 \text{ g cm}^{-2}$ , there is a dead zone that extends from about 0.1 AU to about 6 AU. Note that at small radii, this dead zone is present only at some intermediate values of  $z$ , although the ionizing photons cannot penetrate down to the disk midplane. This is because, if the disk starts turbulent there, the temperature near the midplane is large enough for the gas to be thermally ionized and therefore to remain turbulent. And if the disk does not start turbulent there, the temperature in the dead zone is large enough for thermal ionization to be above the critical level for the onset of the MRI, so that any perturbation will lead to turbulence. From  $r \sim 6$  AU up to about 27 AU, the disk is gravitationally unstable. In this region,  $\alpha_G$  increases with  $r$  from  $10^{-4}$  up to  $10^{-2}$ . The disk is indeed cooler in the outer parts so that, if  $\alpha_G$  were kept constant,  $Q$  would decrease when  $r$  increases. Therefore, to maintain  $Q$  constant,  $\alpha_G$  has to increase with radius. The inner parts of the disk, where the temperature is larger than  $T_i$ , and the surface and outer parts, where the ionizing photons can penetrate, are turbulent. For  $\Sigma_T = 50 \text{ g cm}^{-2}$ , the dead zone extends from  $r \sim 0.2$  AU to  $r \sim 5$  AU and there is no gravitationally unstable region. This is because the dead zone is less extended and less massive than for smaller values of  $\Sigma_T$ . As the ionizing photons can penetrate deeper than in the previous case, the turbulent zone is much more extended.

In this model, there is a range of radii where

the mass of the dead zone is much larger than that of the active layer. We denote  $\Sigma_a$  and  $\Sigma_d$  the column density of the active layer and dead zone, respectively. At  $r = 1$  AU, where the dead zone is vertically very extended, we have  $\Sigma_a/\Sigma_d = 0.6 \times 10^{-2}$  and  $4 \times 10^{-2}$  for  $\Sigma_T = 10$  and  $50 \text{ g cm}^{-2}$ , respectively. Whether hydrodynamic fluctuations driven by the turbulence in the active layers can penetrate down to the disk midplane in that case is not clear.

In order to get a model with higher values of  $\Sigma_a/\Sigma_d$ , we have investigated the case  $\alpha_T = 10^{-2}$  and  $\alpha_D = 10^{-3}$  ( $\dot{M} = 10^{-8} M_{\odot} \text{ yr}^{-1}$  being the same as above). This is close to the values found by Fleming & Stone (2003) in their simulations in which  $\Sigma_a/\Sigma_d$  was varied between 0.187 and 0.75. Figure 2 is the same as figure 1 but with this larger value of  $\alpha_D$ . We note that the range of radii at which the disk is not fully turbulent is the same as before. Here however, there is no gravitationally unstable region. The dead zone being less massive, it remains gravitationally stable. For  $\Sigma_T = 10 \text{ g cm}^{-2}$ , the dead zone now extends from  $r \sim 0.1$  AU up to about 27 AU. The vertical extent of the dead zone is smaller than in the case  $\alpha_D = 10^{-4}$ . At  $r = 0.4$  AU, where the dead zone is the more extended,  $\Sigma_a/\Sigma_d = 10^{-2}$  and 0.1 for  $\Sigma_T = 10$  and  $50 \text{ g cm}^{-2}$ , respectively. This latter value is closer to those investigated by Fleming & Stone (2003). Note that if we were to assume that the Reynolds stress in the midplane were 10% of the Maxwell stress at the boundary of the dead/active zone, as found by Fleming & Stone (2003), we would get  $\alpha_D = 0.03\alpha_T$  after normalizing the stress by the thermal pressure at these locations. But of course the angular momentum flux is spread throughout the different zones and in principle  $\alpha$  should vary with  $z$ .

In figure 3, we plot  $H/r$ ,  $\Sigma$  and the midplane temperature  $T_m$  versus  $r$  for the same parameters as in figures 1 and 2. For comparison, we also plot the curves corresponding to standard disk models (with no dead zone and no adjustment in the gravitationally unstable parts) with constant  $\alpha = \alpha_T$  and  $\alpha = \alpha_D$ . As expected, in the parts where there is a dead zone, the disk is thicker, more massive and hotter. This is because the vertically averaged value of  $\alpha$  decreases as the vertical extent of the dead zone increases, and  $H/r$ ,  $\Sigma$  and  $T_m$  increase as  $\alpha$  decreases (e.g., Frank et al. 1992).

We see that for low values of  $\Sigma_T$ , i.e. when the ionizing photons do not penetrate deep into the disk, the turbulent layer is thin and the properties of the disk at the radii where there is a dead zone are very close to that of a standard disk with constant  $\alpha = \alpha_D$ . For all the values of  $\Sigma_T$ ,  $H/r$  has a maximum at a fraction of or around 1 AU, which produces a puffing up of the disk. This is because the mass density is very high there, so the dead zone is vertically extended, which makes the disk hotter. Note that a maximum is also present in the standard disk models with constant  $\alpha$ . The profiles of  $H/r$ ,  $\Sigma$  and  $T_m$  tend to be a bit steeper than in standard disk models with no dead zone, as they are bracketed by the profiles corresponding to constant  $\alpha = \alpha_T$  and  $\alpha = \alpha_D$  models.

In figure 4, we plot  $\rho$  and  $T$  as a function of  $z/r$  at  $r = 1$  AU for  $\alpha_D = 10^{-4}$  and at  $r = 0.4$  AU for  $\alpha_D = 10^{-3}$  for the same parameters as in figure 3. When the dead zone extends down to the disk midplane, the disk structure is very close to that of a standard disk with constant  $\alpha = \alpha_D$  for the lowest value of  $\Sigma_T$ . For the largest values of  $\Sigma_T$ , the dead zone is small and the disk is similar to a standard disk with constant  $\alpha = \alpha_T$ . For  $\alpha_D = 10^{-4}$ , we actually cannot distinguish between the two models for  $\Sigma_T = 10^2 \text{ g cm}^{-2}$ . We see that the mass density in the dead zone is typically 10 times larger than that of a standard fully turbulent disk with constant  $\alpha = \alpha_T$ .

In figure 5, we plot  $H/r$  versus  $r$  for  $\dot{M} = 10^{-8} \text{ M}_\odot \text{ yr}^{-1}$ ,  $\alpha_T = 10^{-3}$ ,  $\alpha_D = 10^{-5}$  and  $\Sigma_T = 50 \text{ g cm}^{-2}$ , i.e. the same values as above except for lower values of  $\alpha_T$  and  $\alpha_D$ . We checked that decreasing  $\alpha_T$  and  $\alpha_D$  by a factor of ten has almost exactly the same effect as increasing  $\dot{M}$  by the same factor, all the other parameters being kept fixed. When  $\alpha_T$  and  $\alpha_D$  are smaller or  $\dot{M}$  is larger, the disk is more massive and therefore gravitational instabilities develop in a more extended region, up to the disk outer boundary. To keep  $Q$  constant  $\sim 1.6$  there,  $\alpha_G$  has to reach  $2.5 \times 10^{-3}$  in the disk outer parts, i.e. to become larger than  $\alpha_T$ .

We have also run models with  $\alpha_T = 10^{-2}$  and  $\alpha_D = 10^{-3}\alpha_T$ . We get similar results in that case, with the locations where there is a dead zone being hotter, thicker and more massive.

We note that in all the models presented above, the puffing up of the inner parts of the disk casts

a shadow over the outer parts, which therefore do not reprocess stellar radiation. The models presented here are self-consistent in a sense that if the disk is not illuminated by the star to begin with, it will not be able to reprocess the stellar radiation at any time. There may however exist another type of solutions in which stellar irradiation is important. Indeed, if the outer parts of the disk are illuminated at some point (before a steady-state is reached for instance), a flaring is produced that could be maintained. To test this hypothesis, we have modified the surface temperature. Instead of using equation (7) to calculate  $T_s$ , we fix  $T_s = 300 (r/\text{AU})^{-1/2} \text{ K}$ . This corresponds to  $T_s \simeq 950 \text{ K}$ ,  $300 \text{ K}$  and  $\simeq 95 \text{ K}$  at  $r = 0.1, 1$  and  $10 \text{ AU}$ , respectively. These values are close to the surface temperatures computed by D'Alessio et al. (1999) in irradiated disk models for  $\dot{M} = 10^{-8} \text{ M}_\odot \text{ yr}^{-1}$  and  $\alpha = 10^{-3}$ , this value of  $\alpha$  being intermediate between  $\alpha_T$  and  $\alpha_D$ . With this new  $T_s$ , the profile of  $H/r$  we get still shows a shadowing of the outer parts. This suggests that even if the disk outer parts are illuminated by the central star at some point, before a steady-state is reached, they cannot flare enough to remain irradiated after a steady-state is established, so that reprocessing of stellar radiation does not play a role in the steady-state models.

## 5. Discussion and conclusion

In this paper, we have considered a disk in which transport is produced by either: i) Maxwell stress resulting from MHD turbulence in the (gravitationally stable) regions where the gas couples well to the magnetic field; ii) gravitational stress in the parts which are gravitationally unstable; iii) Reynolds stress associated with hydromagnetic waves driven by the turbulence in adjacent layers and Maxwell stress associated with large scale field siphoned off from these turbulent layers in the parts which are not turbulent and are gravitationally stable (dead zones). We have modeled the transport using the Shakura & Sunyaev prescription, with  $\alpha_D$  being 10 to  $10^3$  times smaller than  $\alpha_T$ , and  $\alpha_G$  being adjusted such as to give a Toomre parameter  $Q \sim 1.5$  in the gravitationally unstable regions. Although such a modeling is in principle not valid when the transport is non-local, we believe it does not invalidate the gross

features of the models we have presented.

We have found that steady-state models of such a disk exist, and that they are physically reasonable. Since  $\dot{M} = 3\pi\langle\nu\rangle\Sigma \propto \alpha c_s H \Sigma$ , mass flow through the disk can be uniform only if the disk is more massive, hotter and thicker at the radii where the vertically-averaged value of  $\alpha$  is smaller, i.e. where there is a dead zone. Note that even though the disk is thicker at the locations where there is a dead zone, it remains thin for the parameters investigated here. In disks in which the dead zone tends to be massive, which is the case for the lowest values of  $\alpha_D$  and/or the lowest values of  $\Sigma_T$  investigated here, gravitational instabilities control the dynamics of part of the disk.

Whether these models are realistic or not depends on whether hydrodynamical fluctuations driven by the turbulent layers can penetrate all the way inside the dead zone. This may be more easily achieved when the ratio of the mass of the dead zone to that of the active layer is the smallest, which in our models corresponds to  $\alpha_D/\alpha_T = 0.1$ .

If the disk is at some stage of its evolution out of steady-state, then the surface density will change in such a way as for the disk to evolve toward steady-state. To see this, let us consider a disk in which  $\dot{M}$  decreases inward at some location. Then mass will accumulate there as accretion through this region is slower, until  $\Sigma$  is large enough for the flow to be steady. In contrast, if  $\dot{M}$  increases inward at some location, accretion there will be faster and mass will be depleted until  $\Sigma$  is reduced to the level where a steady-state is reached. The timescale  $t_\nu$  for establishing steady-state at the radii where there is a dead zone may be long though, as it is given by:

$$t_\nu = \frac{r^2}{3\langle\nu\rangle} \sim \frac{1}{3\langle\alpha\rangle} \left(\frac{r}{H}\right)^2 \Omega^{-1},$$

where  $\langle\alpha\rangle = \int_{-H}^H \rho \alpha dz / \Sigma$ . With  $\langle\alpha\rangle = 10^{-2}$  and  $H/r = 0.1$ , we get  $t_\nu \sim 5 \times 10^2$  and  $6 \times 10^3$  years at 1 and 5 AU, respectively, which is much smaller than the disk lifetime. However, if the dead zone at these radii is vertically very extended, we have  $\langle\alpha\rangle \sim \alpha_D$ , so that the viscous timescale can get 100 times longer if  $\alpha_D = 10^{-4}$ . At 1 AU we still get a timescale significantly smaller than the disk lifetime, but this is not the case at 5 AU, where the disk may not be able to reach steady-

state. If these parts of the disk build-up from mass inflowing from further out, then the mass in the dead zone will slowly increase. This process will never produce outbursts as envisioned by Gammie (1999) though. Indeed, before enough mass could pile-up for an outburst to be produced, a steady-state would be achieved in which mass would be transported either by density waves or Reynolds stress driven by the turbulent layers.

Note that the spectral energy distribution of a steady disk such as those considered in this paper is not different from that of a standard disk with no dead zone, as the total flux emitted at the surface depends only on  $\dot{M}$ . The surface temperature also does not depend on  $\Sigma_T$ , as can be seen from equation (7). However, the temperature just below the surface is significantly larger in disks with dead zones than in standard disks. The chemistry there would therefore be different. Grain properties may also differ. To study this, irradiation of the disk by the central star would have to be taken into account. Although it will not be important beyond the regions where there is a dead zone, as these parts are shielded from the stellar radiation due to the puffing up of the disk, it will be important in the parts where  $H/r$  increases.

Finally, we comment that a steady-state disk with a dead zone is a more favorable environment for planet formation than a standard disk, as the dead zone, which in general encompasses the region of planet formation, is significantly more massive. Planet formation would therefore be faster there (Lissauer 1993). Note however that there is an issue as how to stop type I migration of the cores in these dead zones. Turbulence, which has been shown to alter this type of migration (Nelson & Papaloizou 2004), cannot be invoked. But if large scale fields are siphoned off in these regions from the turbulent layers, they may prevent the cores from migrating too fast (Terquem 2003, Fromang et al. 2005, Muto et al. 2008). Planetary cores may also be stopped at the interface between the dead zone and the inner turbulent region, where the surface mass density varies sharply, as suggested by Masset et al. (2006). This process however relies on the (positive) corotation torque becoming dominant over the Lindblad torque due to the density gradient and was studied in the context of a laminar viscous disk. It is not clear how the corotation torque is affected

by the turbulence at the transition between the active and dead zones, and whether it would still be as efficient in this context.

I am grateful to John Papaloizou and Steven Balbus for their comments on an early draft of this paper which led to significant improvements. Part of this work was performed while the author was attending the program *Star Formation Through Cosmic Time* at the Kavli Institute for Theoretical Physics at UCSB, funded by the US National Science Foundation under grant PHY05-51164. I thank the staff and scholars at KITP for their hospitality.

## REFERENCES

- Armitage, P. J., Livio M., & Pringle, J. E. 2001, MNRAS,
- Balbus, S. A., Hawley, J. F. 1991, ApJ, 376, 214
- Balbus, S. A., & Hawley, J. F. 2000, From Dust to Terrestrial Planets, W. Benz, R. Kallenbach & G. W. Lugmair, ISSI Space Sciences Series 9, Kluwer, p. 39
- Balbus, S. A., & Papaloizou, J. C. B. 1999, ApJ, 521, 650
- Bell, K. R., & Lin, D.N.C. 1994, ApJ, 427, 987
- Brandenburg, A., Nordlund, A., Stein, R., Torkelsson, U. 1995, ApJ, 446, 741
- D'Alessio, P., Canto, J., Calvet, N., Lizano, S. 1998, ApJ, 500, 411
- D'Alessio, P., NURIA CALVET,<sup>2</sup> LEE HARTMANN,<sup>2</sup> SUSANA LIZANO,<sup>1</sup> AND JORGE CANTO<sup>1</sup>
- Fleming, T. P., Stone, J. M., & Hawley, J. F., 2000 ApJ, 530, 464
- Frank, J., King, A., & Raine, D. 1992, Accretion Power in Astrophysics, Cambridge Astrophysics Series
- Fromang, S., Terquem, C., & Balbus, S. A. 2002, MNRAS, 329, 18
- Fromang, S., Terquem, C., & Nelson, R. P. 2005, MNRAS, 363, 943
- Fromang, S., & Nelson, R. P. 2006, A&A, 457, 343
- Fromang, S., Papaloizou, J., Lesur, G., & Heinemann, T. 2007, A&A, 476, 1123
- Gammie, C. F. 1996, ApJ, 457, 355
- Gammie, C. F. 1999, Astrophysical Discs, J. A. Sellwood & J. Goodman, ASP Conf. Series, 160, p. 122
- Hawley, J. F., Gammie, C. F., Balbus, S. A. 1995, ApJ, 440, 742
- Igea, J., & Glassgold, A. E. 1999, ApJ, 518, 848
- Kenyon, S. J., Hartmann, L. 1987, ApJ, 323, 714
- Laughlin, G., & Bodenheimer, P. 1994, ApJ, 436, 335
- Lesur, G., & Longaretti, P.-Y. 2007, MNRAS, 378, 1471
- Lissauer, J. J. 1993, ARA&A, 31, 129
- Lodato, G., & Rice, W. K. M. 2004, /mnras, 351, 630
- Matsumura, S., Pudritz, R. E. 2003, ApJ, 598, 645
- Matsumura, S., Pudritz, R. E. 2003, MNRAS, 365, 572
- Masset, F. S., Morbidelli, A., Crida, A., & Ferreira, J. 2006, ApJ, 642, 478
- Nelson, R. P., & Papaloizou, J. C. B. 2004, MNRAS, 350, 849
- Muto, T., Machida, M. N., & Inutsuka, S.-I., 2008, arXiv:0712.1060v2 [astro-ph]
- Papaloizou, J. C. B., & Terquem, C. 1999, ApJ, 521, 823
- Sano, T., Miyama, S. M., Umebayashi, T., & Nakano, T. 2000, ApJ, 543, 486
- Shakura, N. I., & Sunyaev, R. A. 1973, A&A, 24, 337
- Terquem, C. E. J. M. L. J. 2003, MNRAS, 341, 1157
- Turner, N. J., & Sano, T. 2008, arXiv:0804.2916v1 [astro-ph]

---

This 2-column preprint was prepared with the AAS L<sup>A</sup>T<sub>E</sub>X macros v5.2.



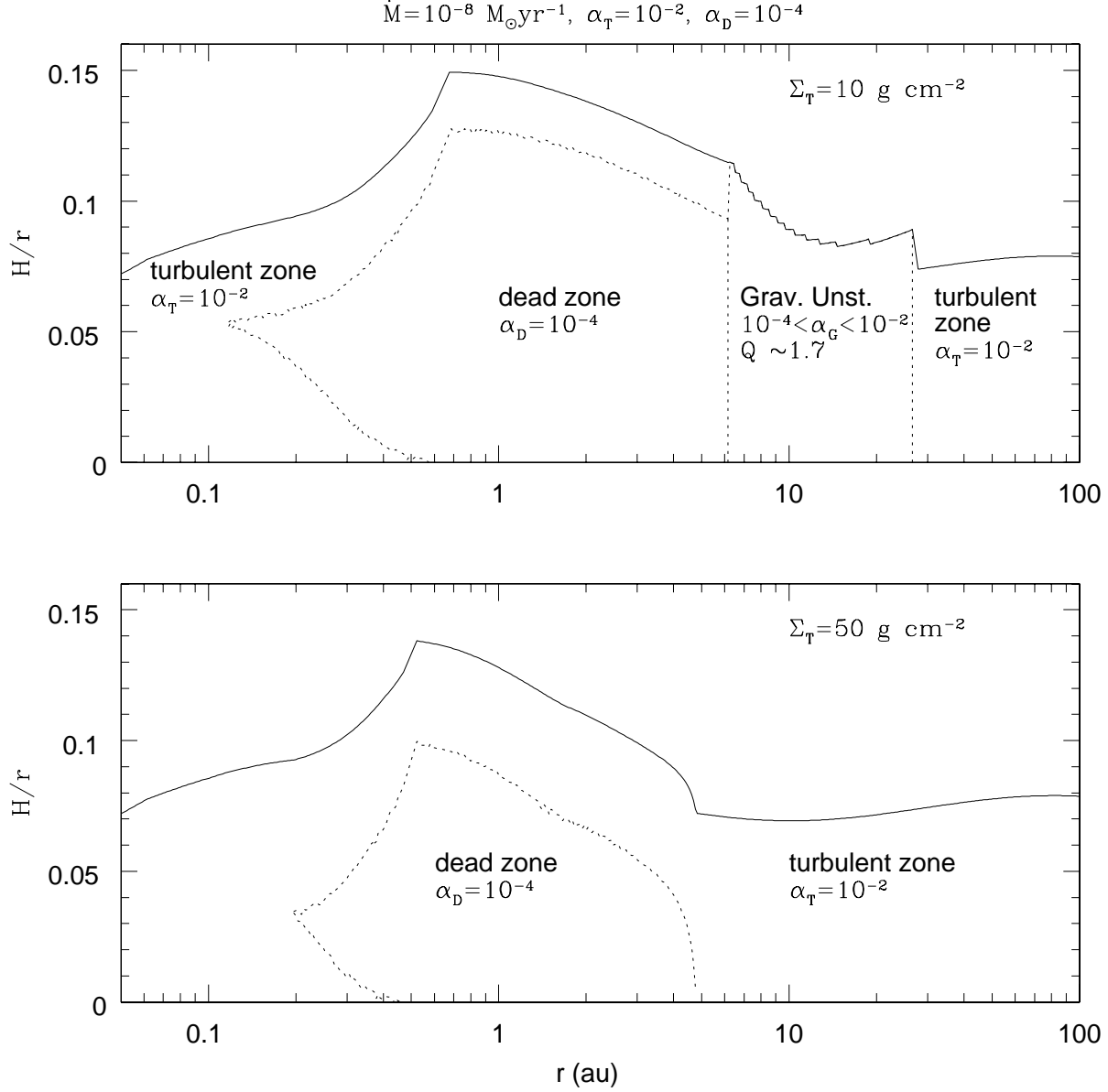


Fig. 1.—  $H/r$  versus  $r$  (in au) for  $\dot{M} = 10^{-8} \text{ M}_\odot \text{ yr}^{-1}$ ,  $\alpha_T = 10^{-2}$ ,  $\alpha_D = 10^{-4}$ ,  $T_i = 10^3 \text{ K}$  and  $\Sigma_T = 10 \text{ g cm}^{-2}$  (*upper plot*) and  $50 \text{ g cm}^{-2}$  (*lower plot*). The solid line delimits the surface of the disk whereas the dotted lines delimit the different regions in the disk. For  $\Sigma_T = 10 \text{ g cm}^{-2}$ , there is a dead zone that extends from  $r \sim 0.1$  au to  $r \sim 6$  au and the disk is gravitationally unstable from  $r \sim 6$  au up to  $r \sim 27$  au. For  $\Sigma_T = 50 \text{ g cm}^{-2}$ , the dead zone extends from  $r \sim 0.2$  au to  $r \sim 5$  au and there is no gravitationally unstable region.

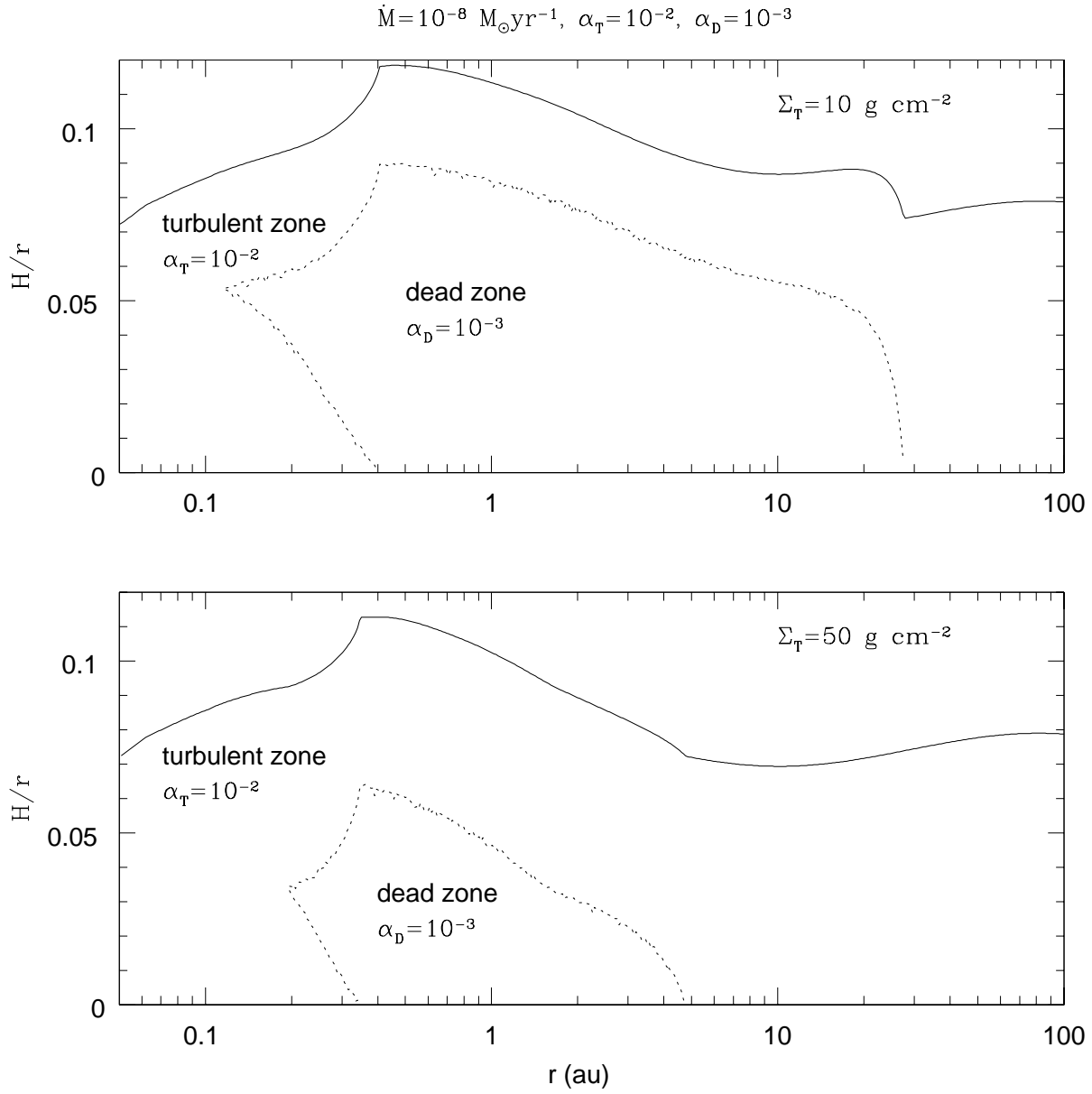


Fig. 2.— Same as Fig. 1 but for  $\alpha_T = 10^{-2}$  and  $\alpha_D = 10^{-3}$ . For  $\Sigma_T = 10 \text{ g cm}^{-2}$ , the dead zone extends from  $r \sim 0.1 \text{ au}$  to  $r \sim 27 \text{ au}$  whereas for  $\Sigma_T = 50 \text{ g cm}^{-2}$ , it extends from  $r \sim 0.2 \text{ au}$  to  $r \sim 5 \text{ au}$ . There is no gravitationally unstable region in that case and the vertical extent of the dead zone is smaller than for  $\alpha_D = 10^{-4}$ .

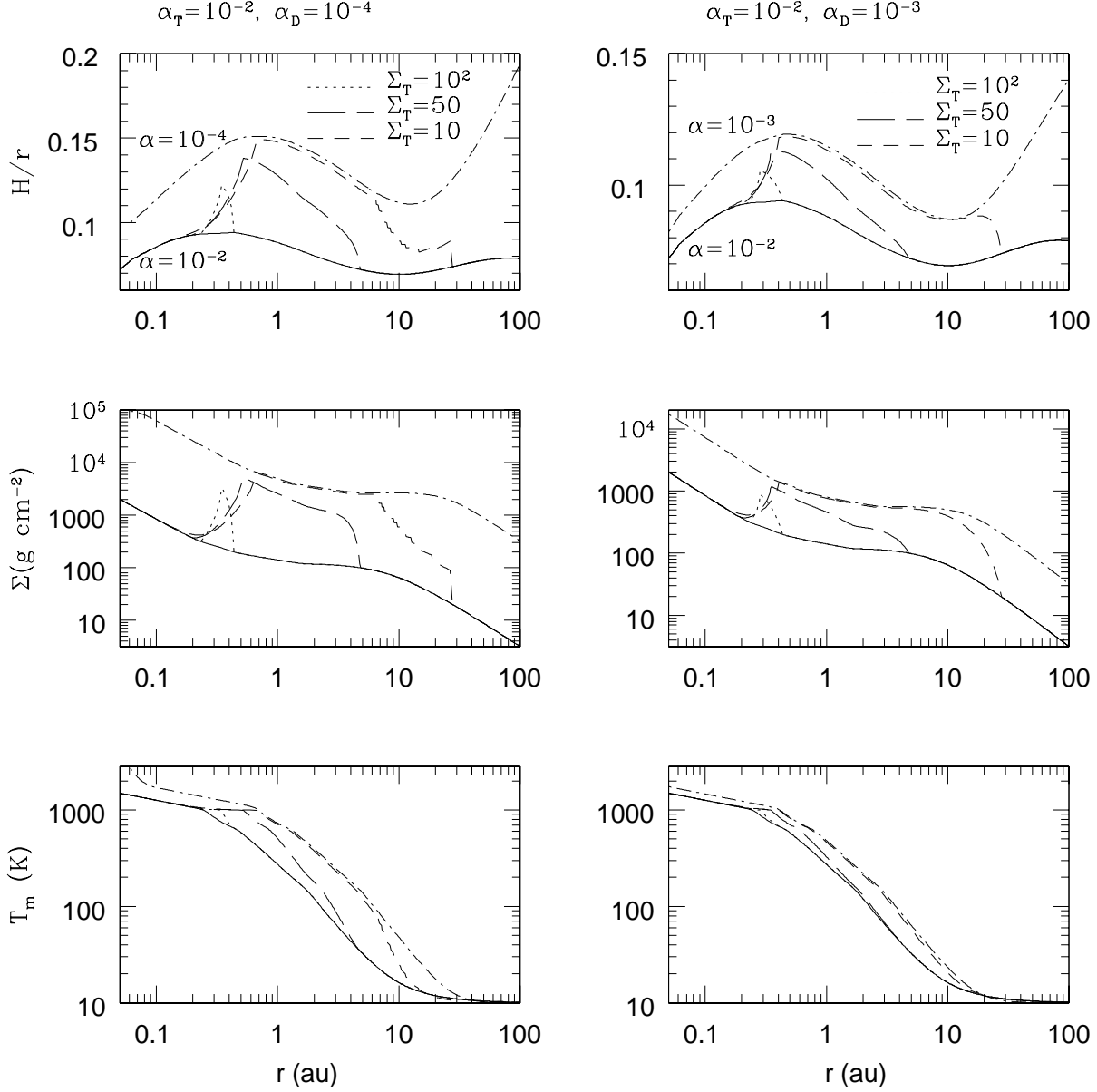


Fig. 3.—  $H/r$  (upper plots),  $\Sigma$  in  $\text{g cm}^{-2}$  (middle plots) and midplane temperature  $T_m$  in K (lower plots) versus  $r$  (in au) for  $\dot{M} = 10^{-8} M_{\odot} \text{ yr}^{-1}$ ,  $\alpha_T = 10^{-2}$  and  $\alpha_D = 10^{-4}$  (left plots) and  $\alpha_T = 10^{-2}$  and  $\alpha_D = 10^{-3}$  (right plots). The solid and dotted-dashed curves correspond to standard disk models (no dead zones) with constant  $\alpha = \alpha_T$  and  $\alpha = \alpha_D$ , respectively. The dotted, long-dashed and short-dashed curves correspond to the disk models with  $\Sigma_T = 10^2$ , 50 and 10  $\text{g cm}^{-2}$ , respectively. In the parts where there is a dead zone, the disk is thicker, more massive and hotter.

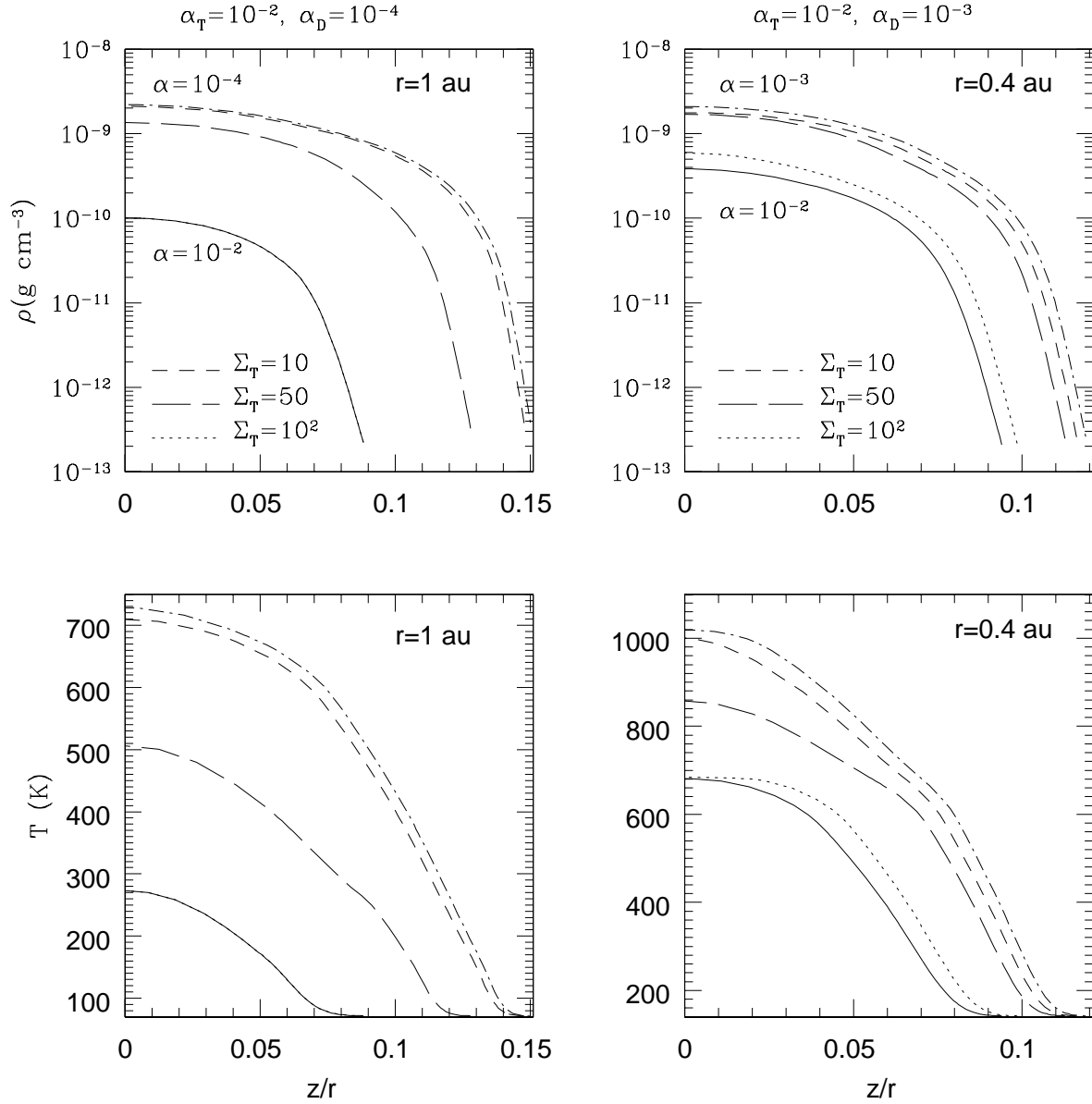


Fig. 4.—  $\rho$  in  $\text{g cm}^{-3}$  (*upper plots*) and  $T$  in K (*lower plots*) as a function of  $z/r$  for  $\dot{M} = 10^{-8} \text{ M}_{\odot} \text{ yr}^{-1}$ ,  $\alpha_T = 10^{-2}$  and  $\alpha_D = 10^{-4}$  at  $r = 1$  au (*left plots*) and  $\alpha_T = 10^{-2}$  and  $\alpha_D = 10^{-3}$  at  $r = 0.4$  au (*right plots*). The solid and dotted-dashed curves correspond to standard disk models (no dead zones) with constant  $\alpha = \alpha_T$  and  $\alpha = \alpha_D$ , respectively. The dotted, long-dashed and short-dashed curves correspond to the disk models with  $\Sigma_T = 10^2$ , 50 and 10  $\text{g cm}^{-2}$ , respectively. On the left plots, the solid and dotted lines are indistinguishable. The vertical structure of the disk depends on the vertical extent of the dead zone.

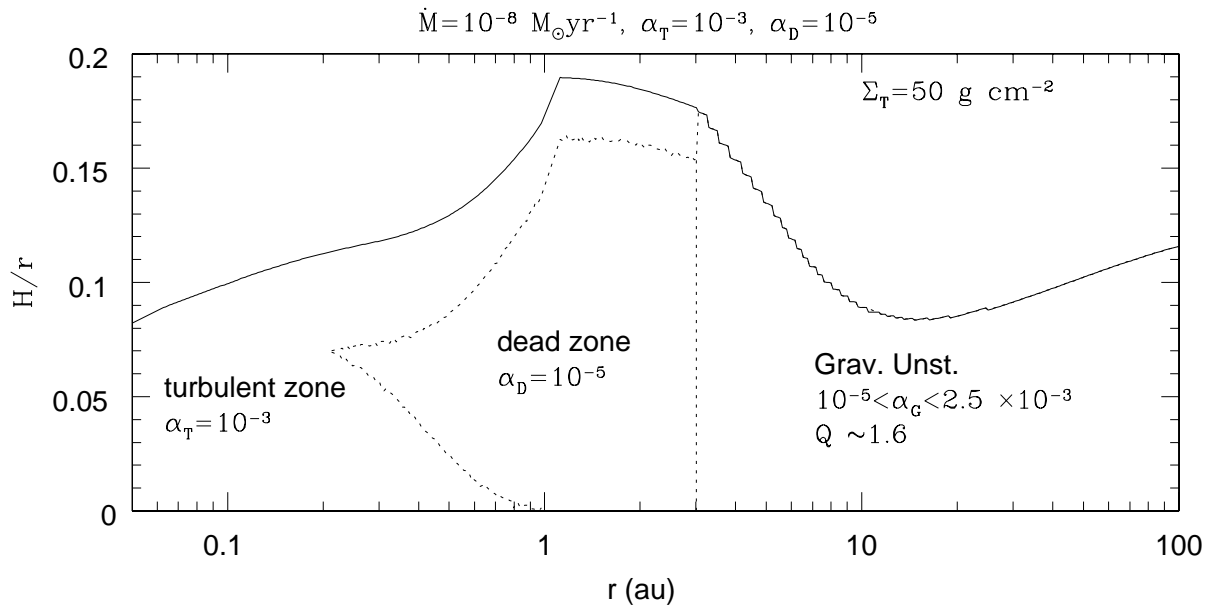


Fig. 5.— Same as Fig. 1 but for  $\alpha_T = 10^{-3}$ ,  $\alpha_D = 10^{-5}$  and  $\Sigma = 50 \text{ g cm}^{-2}$ . Here the disk is gravitationally unstable from  $r \sim 3 \text{ au}$  all the way up to the outer radius.